

# PARTITIONING OF TURBULENT FLUXES OVER DIFFERENT URBAN SURFACES

Andreas Christen<sup>\*</sup>, Christian Bernhofer<sup>\*\*</sup>, Eberhard Parlow<sup>\*</sup>, Mathias W. Rotach<sup>†</sup>, Roland Vogt<sup>\*</sup>

<sup>\*</sup>Institute of Meteorology, Climatology and Remote Sensing, University of Basel

<sup>\*\*</sup>TU Dresden, Institute of Hydrology and Meteorology, Department of Meteorology

<sup>†</sup>Swiss Federal Institute of Technology, Institute for Atmospheric and Climate Science, Zurich

## Abstract

Results from an experimental network of six eddy-covariance stations in and around the city of Basel (Switzerland) are presented. Three sites provide turbulent fluxes over dense urban surfaces (two towers, one parking lot). A suburban site and two rural reference sites with turbulent flux instrumentation complete the setup and allow simultaneous site to site comparison of the energy balance partitioning. The results support previous studies, that over dense urban surfaces also nighttime turbulent fluxes transport always energy away from the surface. Latent heat fluxes and Bowen ratios are highly dependent on the urban vegetation fraction, while storage heat fluxes are coupled with building geometry.

**Key words:** urban energy balance, turbulent fluxes, surface flux partitioning

## 1. SITES AND INSTRUMENTATION

The Basel Urban Boundary Layer Experiment (BUBBLE) is an effort in the frame of COST 715 to increase the understanding of energy exchange and dispersion processes over urban surfaces (Rotach, 2002). As part of the BUBBLE measurements a network of six energy balance sites with eddy covariance instrumentation were operated simultaneously in and around the city of Basel during an intensive operation period (IOP) in summer 2002. The simultaneous operation is a unique opportunity to investigate the partitioning of turbulent fluxes over completely different urban surfaces under the same synoptic forcing. In the last decades a number of energy balance studies were carried out over cities, mostly suburbs (e.g. Grimmond and Oke, 1996), but there is still a lack of knowledge on exchange processes and energy partitioning over dense urban surfaces.

The two urban tower sites (U1 and U2, see Tab. 1 and 2) support a profile of six ultrasonic anemometer-thermometers (sonics) each, one level coupled with a fast hygrometer. The measurements of interest are carried out between two and three times the mean building height  $z_H$ . These two tower sites represent a spatial average over different wind directions of a dense urban surface. The third urban site (U3) was placed very close to the surface over a large 170 by 80 m concrete roof. Another tower was installed over a suburban surface (S1) and two rural reference sites (R1 over grassland, R2 over bare soil) allow direct comparison of the partitioning with the surrounding of the city.

**Tab. 1:** Energy balance sites that are continuously operated during the chosen period from June 10 until July 10. Sites U1 and U2 are long-term sites with observations over 10 months or eight years, respectively.

Site	U1	U2	U3 <sup>(1)</sup>	S1	R1	R2
Name	Basel-Sperrstrasse	Basel-Spalenring	Basel-Messe	Allschwil	Grenzach	Village Neuf
Land use	Urban Tower in and above street canyon, with mainly residential 3-4 storey buildings	Urban Tower above vegetated canyon with mixed, 3-5 storey buildings	Urban EC system over a parking lot on top of a large 26m building.	Suburban Tower in vegetated backyard, residential single and row houses, 2-3 storey	Rural Tower over grassland	Rural EC-System over bare soil
WGS-84	47° 33' 57.2" N 7° 35' 48.8" E	47° 33' 17.6" N 7° 34' 34.6" E	47° 33' 47.6" N 7° 36' 2.6" E	47° 33' 19.0" N 7° 33' 41.5" E	47° 32' 12.0" N 7° 40' 31.5" E	47° 37' 7.6" N 7° 33' 27.1" E
Height a.s.l.	255 m	278 m	255 m	277 m	265 m	240 m
Morphometric Parameters <sup>(2)</sup>	$z_H = 14.6$ m, $\lambda_P = 0.54$ $\lambda_F = 0.37$ $\lambda_C = 1.92$	$z_H = 12.5$ m, $\lambda_P = 0.37$ $\lambda_F = 0.31$ $\lambda_C = 1.75$	$z_H = 18.8$ m, $\lambda_P = 0.41$ $\lambda_F = 0.25$ $\lambda_C = 1.64$	$z_H = 7.5$ m, $\lambda_P = 0.28$ $\lambda_F = 0.12$ $\lambda_C = 1.31$	$\lambda_C = 1$	$\lambda_C = 1$
Vegetation <sup>(3)</sup>	$\lambda_V = 0.16$	$\lambda_V = 0.31$	$\lambda_V = 0.22$ , $\lambda_{V,loc} = 0$	$\lambda_V = 0.53$	$\lambda_V = 0.91$	$\lambda_V = 0.98$

<sup>(1)</sup> Operated from June 24 to July 12 2002 only.

<sup>(2)</sup>  $z_H$ : average building height,  $\lambda_P$ : plan aspect ratio,  $\lambda_F$ : frontal aspect ratio (average over all wind directions),  $\lambda_C$ : complete aspect ratio. Values of U1, U2 and U3 are calculated for a 250m circle around the sites based on 1m raster data of a 3d digital building model without vegetation. Values at S1 were derived from air photo analysis (simplified geometry).

<sup>(3)</sup>  $\lambda_V$ : Vegetation fraction, calculated for a 250m circle around the sites by air photo analysis.  $\lambda_V$  describes the plan area of vegetated surfaces per total plan area. At U3 the local value  $\lambda_{V,loc}$  of the concrete roof is taken into statistics (low sensor height)

<sup>\*</sup> Corresponding author address: Andreas Christen, Institute of Meteorology, Climatology and Remote Sensing, University of Basel, Klingelbergstrasse 27, CH-4055 Basel, Switzerland. e-mail: andreas.christen@unibas.ch

Tab. 2: Instrumentation.

Site	U1	U2	U3	S1	R1	R2
Net radiation $R_n$	1 Net Radiometer K&Z CNR1 (31.7 m, $z/z_n=2.2$ )	2 K&Z CM11 2 Eppley PIR (32.9 m, $z/z_n=2.6$ )	1 Net Radiometer K&Z CNR1 (28 m, 2 m above roof)	1 Net Radiometer K&Z CNR1 (15.1 m, $z/z_n=2.0$ )	2 K&Z CM11 2 Eppley PIR (1.4m)	1 Net Radiometer K&Z CNR1 (2m)
Sensible heat flux $H$	Sonic Gill HS 100/20Hz <sup>(1)</sup> (31.7 m, $z/z_n=2.2$ )	Sonic Metek USA-1 40/20 Hz <sup>(1)</sup> (37.6 m, $z/z_n=3.0$ )	Sonic CSI CSAT 3 60/20 Hz <sup>(1)</sup> (2.2m above roof)	Sonic Metek USA-1 40/20Hz <sup>(1)</sup> (15.8 m, $z/z_n=2.1$ )	Sonic Metek USA-1 20/20 Hz <sup>(1)</sup> (28m)	Sonic CSI CSAT 3 60/10 Hz <sup>(1)</sup> (3.3m)
Latent heat flux $LE$	Coupled with CSI KH <sub>2</sub> O 20 Hz (31.7 m, $z/z_n=2.2$ )	USA-1 with CSI KH <sub>2</sub> O 20 Hz <sup>(1)</sup> (29.9 m, $z/z_n=2.4$ )	Coupled with CSI KH <sub>2</sub> O 10 Hz (2.2m above roof)	Coupled with CSI KH <sub>2</sub> O 20 Hz (15.8 m, $z/z_n=2.1$ )	Coupled with CSI KH <sub>2</sub> O 20 Hz (28m)	Coupled with CSI KH <sub>2</sub> O 10 Hz (3.3m)
Storage heat flux $G$	Residual term	Residual term	Residual term 2 heat flux plates	Residual term	3 heat flux plates 4 soil themistors	3 heat flux plates 4 soil themistors

<sup>(1)</sup>internal sampling rate / output rate

## 2. DATA HANDLING, FLUX CALCULATION AND APPLIED CORRECTIONS

The four components of the radiation balance  $R_n$  were measured at all sites. Radiation instruments were checked and recalibrated after the experiment in an intercomparison with WRC calibrated instruments.

Sensible heat flux  $H$  and latent heat flux  $LE$  are directly derived from eddy covariance measurements of 3d-sonics and humidity fluctuation measurements. The turbulent fluxes are calculated from block averages over one hour without detrending. Flow distortion effects of the sonics are minimized by applying individual 2d-correction matrices derived from wind tunnel investigations. The acoustic sonic temperatures are corrected for crosswind and humidity. Latent heat fluxes are oxygen corrected (Tanner et al., 1993) and the WPL-correction was applied (Webb et al., 1980). The two latter corrections show a relative high impact on  $LE$  at the urban and suburban sites of around +6% (oxygen) and around +10% (WPL), an effect of the high Bowen ratios  $\beta$ .

At the urban sites U1, U2, U3 and the suburban site S1 the storage heat flux  $G$  was determined as residual term. The storage heat flux includes all heat uptake and release of the urban surface materials. The rate of change of sensible heat storage of the air column between the surface and the measurement level is included. However, the results must be treated carefully because, whenever  $G$  is determined as residual term, it incorporates all instrumental and methodical uncertainties. At the rural sites R1 and R2 soil heat flux was measured directly by the mean of 3 heat flux plates and soil temperature measurements. Over the parking lot (U3) two experimental heat flux plates were placed directly above the horizontal concrete surface and provide additional information.

The following sign convention is used: all fluxes directed away from the surface are negative (energy loss), all fluxes towards the surface are positive (energy gain) by using the energy balance equation  $R_n + H + LE + G = 0$ .

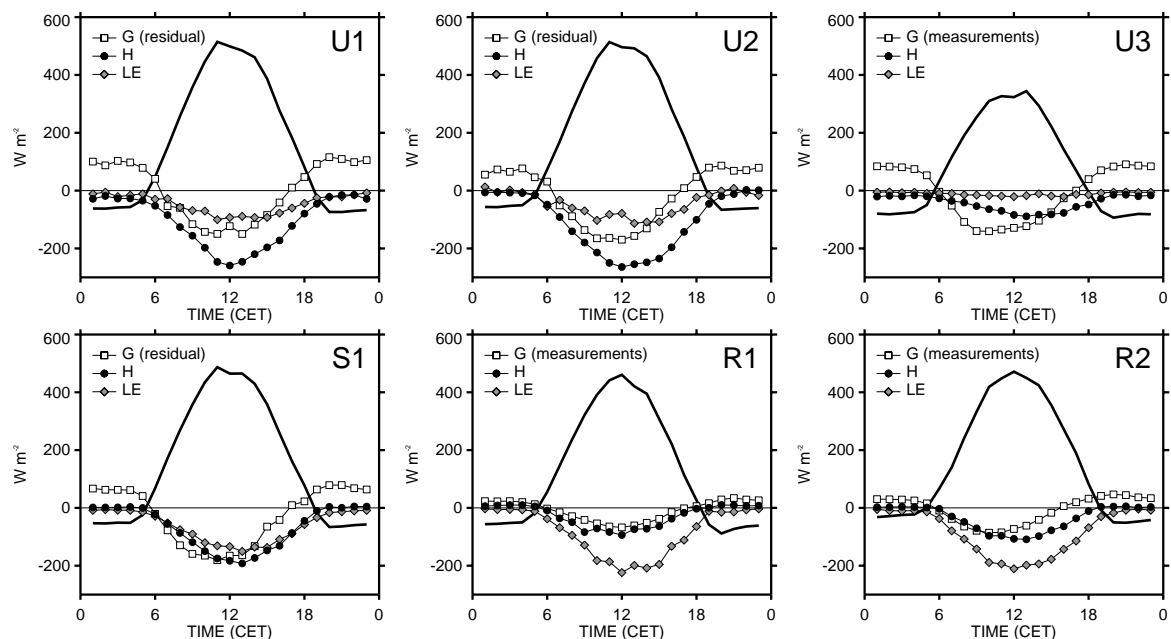


Fig. 1: Average diurnal course over the period June 10 to July 10 2002 of the energy balance components (site codes refer to Tab. 1).

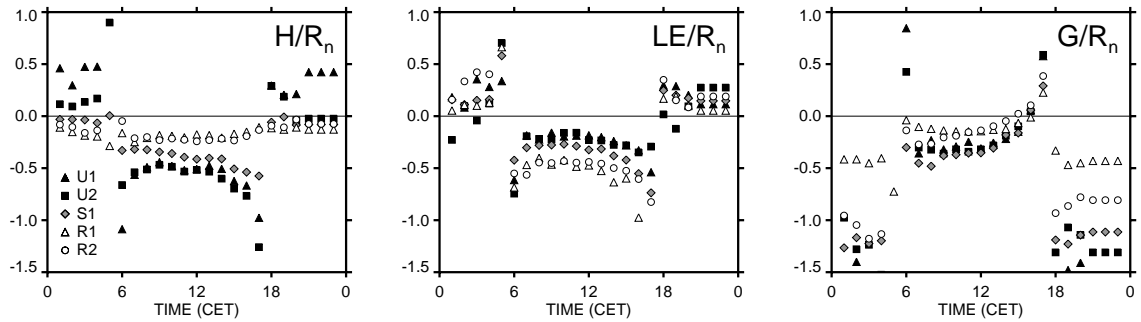


Fig. 2: Diurnal course of the partitioning of the energy balance components  $H$ ,  $LE$  and  $G$  normalized by available net radiation  $R_n$ .

### 3. RESULTS

Results from a summertime period between June 10 and July 10, 2002, are presented. During this period a mean shortwave irradiance of  $22.6 \text{ MJ d}^{-1} \text{ m}^{-2}$ , a mean temperature of  $20^\circ\text{C}$  and  $65 \text{ mm}$  rainfall (mostly thunderstorms) were observed. The period includes 10 clear-sky days. Flux and radiation data are filtered automatically and manually for errors. Heavy rain and dew events were discarded. 65-80% of all situations are taken into analysis.

The high surface per plan area at the built-up sites - described by the complete aspect ratio  $\lambda_c$  - allows additional storage into buildings and leads to storage heat fluxes that are two to three times higher than over flat terrain (Fig. 1, 2 and Tab 3). Surprisingly, the highest  $G$ -values are not reported from the sites with the highest building density. Maximal values are supposed to be around suburban surfaces with a  $\lambda_c = 1.5$  (Fig. 3, middle). An explanation are shading effects. Radiation is dominantly absorbed at roof level.

The daytime storage heat flux shows a pronounced hysteresis by decreasing significantly during the afternoon (see Fig. 3 right).  $G$  gets positive and releases energy to the surface one to three hours before the radiation balance changes sign. This is usually also observed over flat surfaces, but the decrease of  $G$  during afternoon is more pronounced at the urban and suburban sites, because of the higher magnitude of  $G$ , a feature also included in energy balance parametrizations for urban surfaces (Grimmond and Oke, 2002). As a result, the two turbulent fluxes compensate this effect by increasing their intensity continuously towards evening.

A direct effect of the higher storage during daytime is the extremely high nocturnal release of heat at the urban and suburban surfaces (U1, U2, S1). The whole night the release remains higher than the radiative loss. The

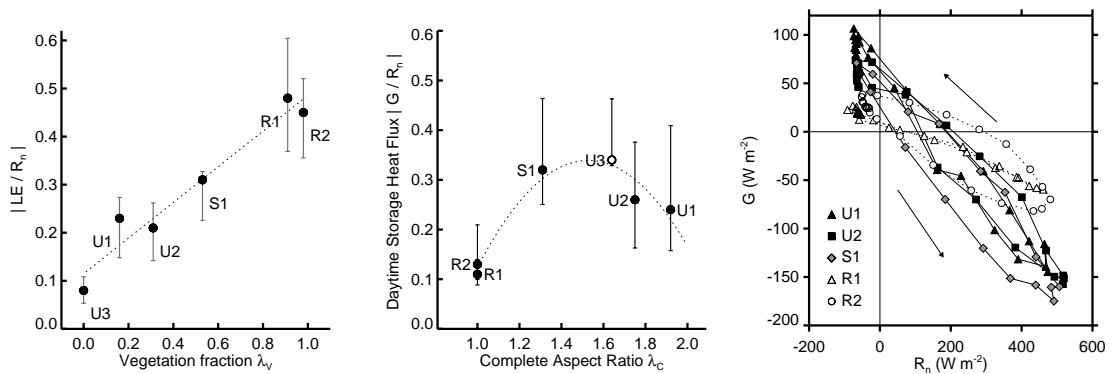
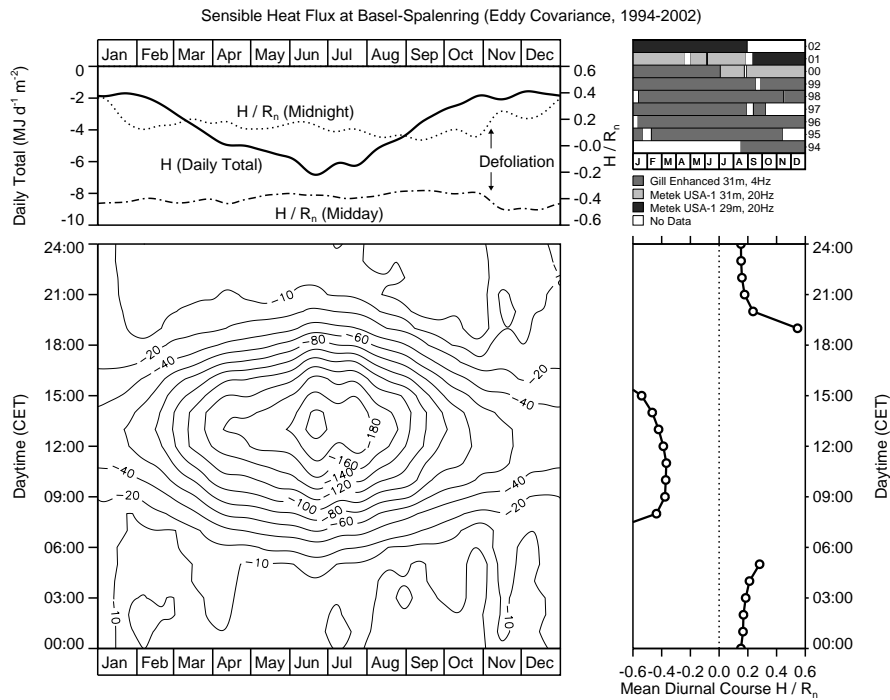


Fig. 3: **left:** Intensity of the daytime latent heat flux  $LE$  compared to the vegetation fraction  $\lambda_v$ . **middle:** Intensity of the daytime storage heat flux  $G$  in dependence of the complete aspect ratio  $\lambda_c$  of the surface. **right:** Mean diurnal hysteresis of the storage heat flux  $G$  vs. Net radiation  $R_n$  flux at the rural and urban sites. The plots show mean values for the period June 10 to July 10 2002. Error bars include 50% of all single 1h-runs.

Tab. 3: Average partitioning of the energy balance during the period June 10 to July 10 2002.

	Day (08:00-16:00), $R_n > 100 \text{ W m}^{-2}$				Night (20:00-04:00), $R_n < -20 \text{ W m}^{-2}$				Daily Total Values in $\text{MJ d}^{-1} \text{ m}^{-2}$			
	$H/R_n$	$LE/R_n$	$G/R_n$	$\beta$	$H/R_n$	$LE/R_n$	$G/R_n$	$\beta$	$R_n$	$H$	$LE$	Albedo
U1	-0.50 ↑	-0.23 ↑	-0.27 ↑	2.32	+0.48 ↑	+0.35 ↑	-1.82 ↓	1.37	+11.5 ↓	-8.2 ↑	-3.8 ↑	11.2 %
U2	-0.49 ↑	-0.21 ↑	-0.26 ↑	2.39	+0.31 ↑	+0.12 ↑	-1.43 ↓	2.25	+13.4 ↓	-8.7 ↑	-3.7 ↑	11.5 %
U3 <sup>(1)</sup>	-0.26 ↑	-0.08 ↑	-0.36 ↑	3.54	+0.23 ↑	+0.09 ↑	-1.33 ↓	2.85	+6.4 ↓	-3.7 ↑	-1.0 ↑	33.5 %
S1	-0.35 ↑	-0.31 ↑	-0.33 ↑	1.25	-0.01 ↓	+0.34 ↑	-1.35 ↓	-0.20	+12.4 ↓	-5.6 ↑	-5.2 ↑	13.1 %
R1	-0.20 ↑	-0.48 ↑	-0.11 ↑	0.43	-0.11 ↓	+0.19 ↑	-0.11 ↓	-0.99	+10.5 ↓	-2.2 ↑	-6.9 ↑	21.7 %
R2	-0.21 ↑	-0.45 ↑	-0.15 ↑	0.50	-0.08 ↓	+0.41 ↑	-0.75 ↓	-0.40	+12.9 ↓	-2.9 ↑	-7.1 ↑	20.2 %

↑ Flux away from surface, ↓ Flux towards surface. Residual terms are in italic type. <sup>(1)</sup> data from June 24 to July 12 2002 only.



**Fig. 4:** Results of the long term eddy-covariance measurements. From 1994 to 2002 different eddy-covariance systems measured sensible heat flux  $H$  at site U2. **Main plot:** The isofluxdiagram illustrates the climatological averaged values of the sensible heat flux  $H$  in dependence of daytime and day of year in  $W m^2$ . The diagram again illustrates that always negative heat fluxes (i.e. away from the surface) are measured – even for nighttime. **Right plot:** Mean diurnal course of the fraction  $H/R_n$  for the period 1994-2002. **Upper left plot:** Yearly course of the daily total values (full line) and fraction  $H/R_n$  for midday and midnight. **Upper right:** Documentation of the different eddy covariance systems that were operated at U2 and contribute to the climatological averaged values.

$G/R_n$  ratio reaches values between 130% and 180% (Tab. 3). In consequence both turbulent fluxes stay negative i.e. away from the surface during night. This is most pronounced at the dense urban sites ( $LE \sim 10$  to 35%,  $H \sim 20$  to 50% of the net radiation). Upward directed sensible heat fluxes during night are observed over the whole year (Fig. 4). At the suburban site the nocturnal  $H$  is nearly zero and energy from storage release is put into  $R_n$  and  $LE$  (higher vegetation fraction). Over the rural surface  $H$  is directed towards the surface, like expected.

It is easily understandable that the lower the vegetation cover, the less latent heat flux is observed (Fig. 3, left). The nocturnal  $LE$ -values stay slightly negative over all surfaces. In the yearly course (Fig. 4) the defoliation of the mostly deciduous urban vegetation leads to a pronounced increase of the sensible heat flux in October / November (dashed curves with  $H/R_n$  in the upper plot of Fig. 4). The higher wintertime  $H$  values are best explained by the change of  $\beta$ . But the effect of anthropogenic heating is still unknown. Wintertime  $H/R_n$  of up to 0.6 are measured at U1 during the BUBBLE wintertime observations (Christen et al. 2002).

#### 4. ACKNOWLEDGEMENTS

The Swiss Federal Office for Education and Science provides funding of this study (# C00.0068). Indiana University and the Bulgarian National Institute of Meteorology and Hydrology provided additional instrumentation.

#### 5. REFERENCES

Christen, A., Vogt, R., Rotach, M. W., Parlou, E., 2002, "First Results from BUBBLE II: Partitioning of turbulent heat fluxes over urban surfaces". *Proc. of 4th Sym. Urban Environ. Norfolk VA*. pp 137-138

Grimmond, C. S. B., Oke, T. R., 2002, "Turbulent heat fluxes in Urban areas: observations and a local-scale urban meteorological parametrization scheme (LUMPS)". *J. Appl. Meteor.*, **41**, p. 792-810

Grimmond, C. S. B., Oke, T. R., 1995, "Comparison of heat fluxes from summertime observations in the suburbs of four north American cities". *J. Appl. Meteor.*, **34**, p. 873-889

Rotach, M.W., 2002, "Overview of the Basel Urban Boundary Layer Experiment" *Proc. of 4th Sym. Urban Environ. Norfolk VA*. pp 25-26

Tanner, B. D., Swiatek, E., Greene, J. P., 1993: "Density fluctuations and use of the Krypton Hygrometer in surface flux measurements". *Management of irrigation and drainage systems, July 21-23, 1993, Park City, UT*. pp 945-952.

Webb, E., Pearman, G., Leuning, R., 1980, "Correction of flux measurements for density effects due to heat and water vapour transfer", *Quart. J. Roy. Meteorol. Soc.*, **106**, pp 85-100.